# SOIL GAS ANALYSES AS INDICATOR OF FAULT ZONES – EXAMPLES FROM THE TAUPO VOLCANIC ZONE

Egbert Jolie[1], Anna Jentsch[1], Fátima Rodríguez[2,3], Gladys Melián[2,3], Andrew Rae[4], Agnes Mazot[4], Mark Harvey[4], Nemesio M. Pérez[2,3]

[1] International Centre for Geothermal Research, Helmholtz Centre Potsdam, GFZ German Research Centre For Geosciences,

Public Law Foundation State of Brandenburg, Telegrafenberg, 14473 Potsdam, Germany

[2] Environmental Research Division, Institute of Technology and Renewable Energies (ITER), 38611 Granadilla de Abona, Tenerife, Canary Islands, Spain

[3] Instituto Volcanológico de Canarias (INVOLCAN), 38400 Puerto de la Cruz, Tenerife, Canary Islands, Spain

[4] School of Environment, University of Auckland, New Zealand

jolie@gfz-potsdam.de

**Keywords:** *Fault zone analysis, diffuse degassing, emanations, fracture permeability.*

## ABSTRACT

Different analytical approaches to measuring diffuse soil gas emissions were tested for their capability to indicate permeable fault segments in areas with and without obvious geothermal manifestations on the surface environment. The methods were applied in three active normal faulting regions in the Taupo Volcanic Zone (Reporoa, Ngapouri, Maleme). Gases such as carbon dioxide and radon are proven tracers for geothermal subsurface activity (Chiodini et al., 1998; Giammanco et al., 2007). Hence, an increase in emissions across and close to faults could be indicative for permeable fracture zones bearing geothermal fluids.

Carbon dioxide efflux and concentration measurements were performed using the accumulation chamber method and an open-path Tunable Diode Laser (TDL), respectively. Furthermore, radon and thoron activity measurements in soil gas have been performed by alpha spectroscopy. Gamma spectroscopy was used as a complementary method to detect solid nuclides (e.g., $^{214}Bi$, $^{208}Tl$) originating from radiogenic minerals in the subsurface. Additionally, an extended soil gas survey was performed in one of the study areas by taking soil gas samples and performing chemical analyses (e.g., He, Ar, Ne, $H_2$, $N_2$, $O_2$, $CH_4$) by Quadrupole Mass Spectrometry (QMS) and micro-Gas Chromatography (μGC), as well as carbon isotopic analysis of the soil gas $CO_2$ ($\delta^{13}C$-$CO_2$) by an Isotopic Ratio Mass Spectrometer (IRMS).

A further objective of this study was the comparison of different methods on structural-geological questions and their correlation to each other. Preliminary results suggest that the combination of different techniques provides a comprehensive understanding of the fluid migration along fault zones and in geothermal systems; however, the correlation between different parameters requires additional investigation.

## 1. INTRODUCTION

### 1.1 Fault zone analysis

The development of geothermal reservoirs for direct or indirect utilisation requires detailed understanding of the subsurface geology in particular structural characteristics. Hence the analysis of fault zones is not only of scientific, but also of economic interest. Surface studies that include detailed geological mapping, and various geophysical surveys, provide important information about structural properties of a fault, such as vertical offset or displacement rates. The use of different in-situ techniques for the assessment of diffuse degassing processes provides an overall picture regarding spatial and temporal changes in fault permeability. Herein, different questions have been addressed to the different sites.

### 1.2 Diffuse degassing processes

Diffuse degassing processes are used to monitor active volcanic areas where continuous measurement of gas fluxes (e.g. $CO_2$, $H_2S$, $^{222}Rn$) provides important input to volcanic hazard analysis. In particular soil $CO_2$ efflux measurements are widespread in different geoscientific disciplines, such as volcano and environmental monitoring. Herein, we intend to use increased gas emissions as an indicator of structural permeability along fault zones (Jolie et al., 2016), e.g., between Reporoa and Waiotapu.

Elevated gas fluxes away from active volcanic centers are also possible where deep reaching faults act as preferential pathways for magmatic or geothermal gases (Lee et al., 2016). Studies in tectonically active areas, e.g., Apennines (Chiodini et al., 2004) or Basin and Range Province (Jolie et al., 2015) have shown that significant amounts of $CO_2$ can be emitted. From the perspective of geothermal resource evaluation, the mapping of geothermal gases across active fault lines is important to understand the properties of a fault (e.g., permeability), and hence their potential as a well target, as well as understanding the structural-geological characteristics.

### 1.3 Geological setting and study areas

The Taupo Volcanic Zone (TVZ) is located on the North Island of New Zealand and is recognised as one of the most productive areas of Quaternary silicic volcanism in the world. Intense volcanism as well as geothermal surface manifestations follow the rifting arc structure resulting from the back-arc extension of the Australian plate (Wilson and Rowland, 2015). Due to the oblique subduction of the Pacific plate towards the west beneath the Australian plate (Rowland and Simmons, 2012; Lamb and Smith, 2013), the annual extension rate across the TVZ is up to 15 mm; consequently a dense system of active normal faults developed (Fig. 1) (Rowland et al., 2010; Villamor and Berryman, 2001). The Taupo Fault Belt (TFB) named by Grindley (1960) also referred to as the Taupo Rift is the surface expression of rift related faulting and extends from the Bay of Plenty coast in the northeast to Mt Ruapehu, an andesitic stratovolcano (Kilgour et al., 2013) in the southwest. Predominantly active normal faults within the rift, which has a maximum width of 40 km, have opposing northwest- and southeast- facing fault dips that define the rift axis. The largest fault displacements (1-2 km) occur along the eastern rift margin (Rowland and Sibson, 2001; Seebeck et al., 2014). The beginning of the convergence of the Pacific plate beneath the Australian plate dates from ~16Myr ago (Wilson and Rowland, 2015).

Although the majority of faults in the TFB can be traced using aerial photographs, digital elevation models, as well as detailed geological surface mapping, it is often difficult to distinguish fault scarps due to their being covered by relatively young volcanic successions. Faulting varies spatially and temporally. Towards the rift margins the faults tend to be longer and continuous (e.g. 20-30 km) and cut through volcanic surfaces and basement metasedimentary rocks. Whereas dense networks of short segmented faults (e.g. 1-4 km length) are observed towards the rift axis displacing young volcanic and fluvial deposits (Seebeck et al., 2014; Villamor and Berryman, 2001; Grindley 1960). Faults have the capability to be hydraulic as well as gas conductors connecting shallow and deep geological environments. This mainly depends on the permeability of a fault, which is influenced by structural properties (e.g., slip rate), the temporal evolution of a fault zone, the mechanical properties of the displaced lithologies and state of stress (Smith et al., 1991). In geothermal systems faults can be preferential targets for exploration and production of the reservoir, since they often act as major conduits (i.e., upflow zones) for hot fluids and gases (Bense et al., 2013; Caine et al., 1996).

Three study areas have been selected for the application of different techniques to measure diffuse degassing and emanations at Earth's surface (Fig. 1).

### 1.3.1 Reporoa

The Reporoa geothermal system is a NE-SW elongated basin located to the South of Waiotapu, the largest geothermal field in the Taupo Volcanic Zone (Giggenbach et al., 1994). The Paeroa Range in the northwest and the Kaingaroa Plateau in the southeast define the areal extent of the basin. Nairn et al. (1994) described the Reporoa depression as a caldera and the source for the Kaingaroa Ignimbrites which were deposited as a rhyolitic pyroclastic flow 0.24 Ma ago. Although there is no obvious fault scarps at the surface it is known that inferred normal faults occur in the area and are possible pathways for hydrothermal fluids (Bignall, 1990). It has been debated whether the Reporoa system is geohydrologically linked to the Waiotapu system (Healy and Hochstein, 1973), or if Reporoa comprises an individual geothermal system (Hedenquist and Browne, 1989).

### 1.3.2 Ngapouri

The normal Ngapouri Fault is a major splay of the Paeroa Fault, and with a strike of 55° follows the dominant structural (40°-60°) of the TFB (Rowland and Sibson, 2001; Villamor and Berryman, 2001; Nairn, 1973). It has a scarp length of about 15 km with a downthrown northwestern block. The fault passes from the Paeroa Trig in the south close to the Paeroa Fault, along the hummocky sloped terrain of the Paeroa Range (Newson et al., 2002) to the eastern shore of Ngapouri Lake, towards the northeast passing west of the Waiotapu geothermal area and beyond past Lake Okaro in the north (Grindley, 1963). Along this strike length it crosses the two dacite volcanoes Maungakakaramea (Rainbow mountain) and Maungaongaonga (Hedenquist and Henley, 1985). In the south, two distinct fault lineaments mapped by Villamor and Berryman (2001) merge beneath a small knoll of ignimbrite (Leonard et al., 2010). Areas of steaming ground and fumarolic activity are situated at the southern end of the fault and also towards the north on the lower flanks of Maungaongaonga. The Ngapouri Fault scarps are typically poorly preserved due to partial burial by recent ash, but the alignment of several hydrothermal explosion craters along its length and the areas of geothermal activity aid definition of the surface trace (Healy, 1974; Hedenquist and Henley, 1985; Villamor and Berryman, 2001). A previous study on several excavated trenches across Ngapouri Fault provides estimates of vertical offsets and displacement rates (0.23 ± 0.001 mm/yr) of the > 0.23 Ma ignimbrites (Villamor and Berryman, 2001; Berryman et al., in prep.).

### 1.3.3 Maleme

The Maleme Fault Zone (MFZ) is a complex network of up to 16 fault strands that form a 2.5 km wide central axis to the TFB. The steeply (~75°) dipping faults splay and merge at different positions and vary their general trend from 55° in the south to 35° in the north over a 19 km long section. Sequences of lacustrine and young volcanic deposits are displaced by about 3.55 ± 0.3 mm/a over the past 20000 years. In the northern part of the MFZ, scarp heights can be between 1-15 m high (Villamor and Berryman, 2001; Tronicke et al., 2006).

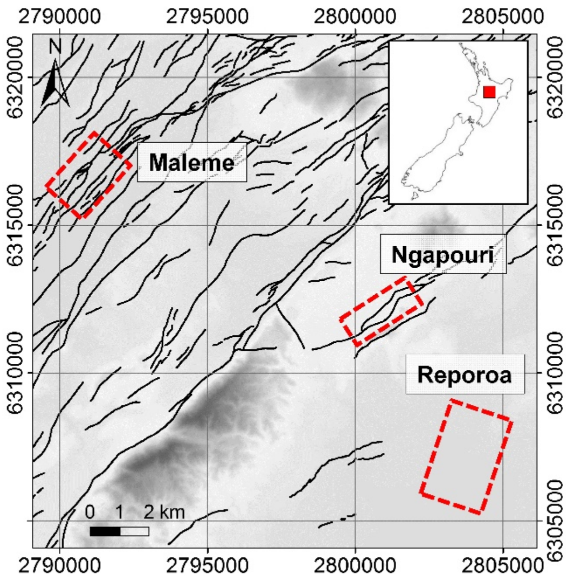


**Figure 1: Topographic map with three survey sites (red rectangles) and mapped active faults (black lines, source: GNS Science active fault database).**

## 2. METHODS

Seven different methods have been applied at the selected study areas during field surveys in June/July 2014 and from October 2015 to February 2016. Measurements have been arranged as regular grids (point spacing ranging from 25-100 m) or single profiles perpendicular to major fault orientation.

### 2.1 Accumulation chamber

Measurements of diffuse $CO_2$ emission rates were performed in-situ according to the accumulation chamber method (Parkinson, 1981). For this study a portable fluxmeter with a LICOR LI-820 single path, dual wavelength, nondispersive infrared carbon dioxide analyser was used (West Systems Ltd., 2002) with a measurement range of 0-20,000 ppmV (optical bench 14 cm). The LICOR analyser is interfaced to a hand size computer running the data acquisition software. Measurement procedure consists of placing the chamber on the ground, obligating to recirculate the gas in a close loop between the chamber and the analyser. In the hand size computer, the increase of $CO_2$ concentration as a function of time is recorded, allowing the operator to calculate the $CO_2$ efflux at each measuring site. To verify the performances and the reliability of this method, several calibration tests were made in the laboratory and the accuracy was estimated to be ±10%.

### 2.2 Tunable diode laser (TDL)

The tunable diode laser spectroscopy (TDLS) technique consists of the measurement of gas mixing ratio based on the absorption of Infra-Red radiation by the target gas. The TDL used in this study consists of a GasFinder 2.0 Tunable Diode Laser (Boreal Laser Inc), an Infra-Red transmitter/receiver (transceiver) unit that can be used to measure $CO_2$ mixing ratios over linear paths of up to 1 km distance. A laser light emitted from the transceiver propagates through the atmosphere to a retro-reflector array and returns to the transceiver where it is focused onto a photodiode detector. These two signals are converted into electrical waveforms. A computer inside the transceiver is processing these waveforms to determine the actual concentration of $CO_2$ (ppmv) with an accuracy of ± 2% (Trottier et al., 2009). The computed gas concentration is shown on the back panel of the monitor and a laptop connected to the transceiver can display and store the data (Myers et al., 2000). It is a portable tool that has been used for monitoring $CO_2$ degassing in volcanic areas where we usually find really high concentration of $CO_2$ (Mazot and Christenson, 2012).

### 2.3 Alpha spectroscopy

Radon $^{222}$Rn and thoron $^{220}$Rn activity concentration in soil gas samples have been determined by a radiometric in-situ measurement of their short living radon daughter products ($^{218}$Po and $^{216}$Po), which emit alpha radiation at nuclide specific energies. The number of the detected $^{218}$Po and $^{216}$Po ions per time unit is proportional to the radon, respectively thoron activity concentration in the measurement chamber (Jolie et al., 2012). Two portable Sarad RTM2200 monitors have been used. Increased radon $^{222}$Rn activity concentration can be correlated with deep fracture zones.

### 2.4 Gamma spectroscopy

Gamma radiation was determined with a Sarad RTM 2200 monitor, connected to a sodium iodide scintillator (NaJ(TI)) and coupled with a photomultiplier (PMT) to increase the signal strength. Scintillation detectors convert radiation energy into light, which is converted again into electrical signals. The device is capable of recording the complete gamma spectrum from 0-2,850 keV. The gamma radiation of three characteristic solid nuclides with significant spectral peaks ($^{214}$Bi, $^{208}$Tl, $^{40}$K) was determined to deduce the local dose rates (Jolie et al., 2012). $^{214}$Bi and $^{208}$Tl are indicative of deep-reaching fracture zones.

### 2.5 Quadrupole Mass Spectrometry (QMS)

At each measurement site in the Reporoa area, soil gases samples were collected at ~40 cm depth using a metallic probe following the method described by Hinkle and Kilburn (1979) to have the chemical and isotopic composition of the soil gas. The samples were stored in 10 ml glass VacutainerTM vials with rubber stoppers. The probe was flushed by drawing 20 ml through it before the gas sample was inserted into glass vials. Another needle is inserted through the septum in order to allow the internal gas to escape when the gas sample is introduced

Soil He, $^{40}$Ar and $^{36}$Ar concentration was analysed within 24 h by means of a Quadrupole Mass Spectrometer (Pfeiffer Omnistar 422) using atmospheric air as standard for calibration. The quadrupole mass filter consists of four parallel rods arranged in a particular geometry with opposite electrical potential. Ions created through electron bombardment in the ion source are separated by the mass/charge ratio in the rod system and a mass spectrum is obtained by monitoring the ions passing through the quadrupole filter. He is analysed with high precision with this instrument (±0.3 ppm).

### 2.6 Micro-Gas-Chromatography (µGC)

Soil $CO_2$, $CH_4$, $H_2$, Ne, $O_2$ and $N_2$, concentrations were analysed within 24 h by means of a double column VARIAN 4900 micro-Gas Chromatograph (micro-GC). Soil gas samples were collected in the Reporoa area as explained in section 2.5. The instrument was previously calibrated with certified standard gases of known composition. The analysis of He, $H_2$, $O_2$, Ne and $N_2$ was performed with a Thermal Conductivity Detector (TDC), equipped with a 20 m length Molsieve 5Å column and pure Ar as carrier gas. The concentrations of $CO_2$ and $CH_4$ were determined using a Poraplot-Q column of 10 m length, a TDC detector and pure Ar as carrier gas. The precision of the instrument was estimated to be 5%, while the detection limit was calculated to be 0.3 ppm for $H_2$, 1.5% and 1.5 ppm for Ne, 0.1% and 15 ppm for $O_2$, 0.1% and 50 ppm for $N_2$ and 2% and 10 ppm for $CO_2$.

### 2.7 Isotopic Ratio Mass Spectrometer (IRMS)

Soil gas samples at each measurement site of Reporoa were collected following the method described at 2.5 section to determinate the isotope composition of carbon in soil gas $CO_2$. Carbon isotopic analysis of the soil gas $CO_2$ ($\delta^{13}$C-$CO_2$) was analysed by isotopic ratio mass spectrometry (IRMS) with a Finnigan MAT Delta S and Thermo Finnigan MAT 253 mass spectrometers at the Fluid Laboratory of ITER, Spain. The $^{13}$C/$^{12}$C ratio is given as $\delta^{13}$C-$CO_2$ values with respect to VPBD standard with an uncertainty of ±0.1‰. GasBench II was used to introduce the soil gas into the Thermo Finnigan MAT 253. The gas injection system uses a two port needle which adds a gentle flow of helium into the sample vial to displace the sample gas.

## 3. PRELIMINARY RESULTS

Dependent on the scientific question an individual measuring approach was developed for each study area (Table 1).

**Table 1: Overview of scientific focus for each study area.**

| Study area | Main focus | Applied technique |
|---|---|---|
| Reporoa | Geohydrological link between Reporoa and Waiotapu geothermal system | Acc. chamber, Alpha-/Gamma spectroscopy, QMS, µGC, IRMS |
| Ngapouri | Permeable segments of fracture zones; Fault mapping | TDL, Acc. chamber, Alpha-/Gamma spectroscopy |
| Maleme | Variation of degassing processes from rift axis to margin | Acc. chamber, Alpha spectroscopy |

### 3.1 Site-specific measuring approach

#### 3.1.1 Reporoa

Our study undertakes analyses of surface degassing as transects across the basin to evaluate whether a geohydrological link can be discerned between the Waiotapu geothermal field and the Reporoa system. The study area has a dimension of 5.3 km (NE-SW) x 1.6 km (NW-SE). Sampling sites have been arranged in a regular grid of NE-SW orientation with variable point spacing dependent on the measurement technique. $CO_2$ and soil gases were measured at a spacing of 100 m x 135 m, whereas $^{222}Rn$ was measured at 100 m x 270 m spacing. Gamma radiation was measured along NW-SE profiles with a spacing of 120 m between profiles.

#### 3.1.2 Ngapouri

Both $CO_2$ efflux, $CO_2$ concentration and $^{222}Rn$ activity concentration measurements were applied at the Southern segment of the fault between areas of geothermal surface activity. Some preliminary results were reported previously by Mazot et al. (2014). In total ten profiles, each between 500-1,000 m long are crossing the two fault lines perpendicular to their strike. The NE-SW extension of the study area is ~3 km with NW-SE trending profiles. The purpose of the study is to test whether geothermal-derived $CO_2$ can also be detected along splays of the Ngapouri Fault where no obvious geothermal surface activity is observed. With the measurement of surface degassing processes across Ngapouri Fault it could also be assessed whether there is a possible linkage between the Waiotapu-Waikite geothermal system, extending in depth to the south along Ngapouri Fault.

#### 3.1.3 Maleme

Six traverses across several fault strands were chosen to measure radon/thoron activity concentrations and carbon dioxide efflux. The aim was to cover as many fault strands as possible to see a change in gas anomalies from the tectonically most active part-the graben axis towards the west-out of the graben. Additionally, it was of interest to understand whether some of the fault strands are linked to each other in the subsurface where no surface expression is visible.

### 3.2 Preliminary results

Preliminary results (Jentsch et al.; Jolie et al.; in prep.) indicate that high gas fluxes can be measured in areas where no obvious geothermal surface activity is observed. This is useful in particular for an improved understanding of a geothermal system and the interaction between different geothermal systems. Additionally, detected anomaly pattern can also be used as a basis for mapping permeable segments of fracture zones.

Measurements across several fault strands at Maleme Fault Zone show partly elevated $CO_2$ efflux values and $^{222}Rn$ activity concentrations at the top of the fault scarps. Most efficient approach in the detection of degassing anomalies at Earth's surface are raster based measurements. Even larger sampling site spacings, as applied for $CO_2$ at Reporoa (100 m x 135 m), enable the detection of geothermal anomalies at sufficient resolution.

Radon measurements at Reporoa helped to identify and map parts of a potential outflow zone from the Opaheke Hot Springs. The different anomaly behavior of $^{222}Rn$ and $CO_2$ (see exemplary data set; Fig. 2) is likely to be caused by the impact of surface geology (i.e., sinter deposits). Preliminary results from Ngapouri also show a different behavior of $^{222}Rn$ and $CO_2$, and site-specific explanations still have to be found for each anomaly. In general, radon anomalies can also be caused by in-situ rock rather than gas migrating along fault zones. Therefore, surface geology always has to be taken into account for the interpretation. We intend to develop a comprehensive understanding of the complex data set for Reporoa (Table 1). This will be useful for the further development of a gas fingerprint for different geothermal systems (Jolie et al, 2016).

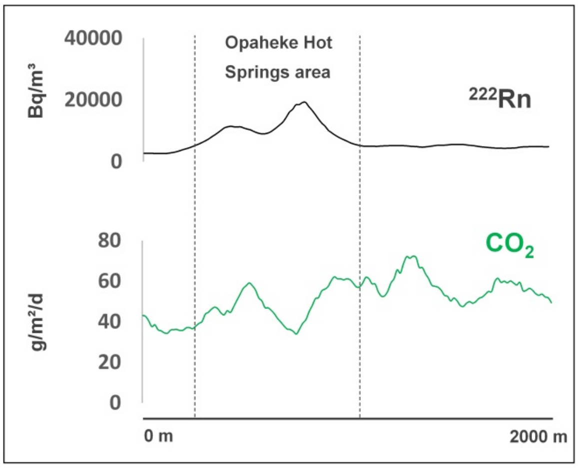


**Figure 2: Anomaly pattern of $^{222}Rn$ and $CO_2$ along a 2 km NW-SE profile across the Opaheke Hot Springs.**

Gamma radiation measurements have been applied at Reporoa with promising results. By the application of the roving principle (Jolie et al., 2015) the subsurface continuation of geothermal surface manifestation could clearly be detected. The application of this approach is still new in geothermal exploration and has so far only been tested in the Basin-and-Range Province (Jolie et al., 2016), the East African Rift System/Ethiopia (Jolie et al., in prep.) and in the Taupo Volcanic Zone (this study).

## 4. CONCLUSION

This paper presents a methodological approach of a full soil gas survey which was applied for the first time in the Taupo Volcanic Zone. Three key sites of different geological characteristics have been selected. Preliminary results from the different study areas indicate that surface degassing and emanation measurements are useful techniques to assess and identify permeable fault segments.


## ACKNOWLEDGEMENTS

We thank the local Maori Trust for the permission to carry out this survey. Thanks also to the local farmers who gave access to their land. We also thank Pilar Villamor for discussions about the structural geology of selected field sites; Cecilia Rodriguez-Gomez and GNS technician Nick Macdonald for assistance during field work. Special thanks are addressed to Chris Bromley for guidance and interesting discussions throughout the survey.


## REFERENCES


Bense, V.F., Gleeson, T., Loveless, S.E., Bour, O., Scibek, J.: Fault zone hydrogeology. *Earth Science Reviews;* 127, pp. 171-192. (2013).

Bignall, G.: Hydrology and hydrothermal alteration, Reporoa well (1), Reporoa, New Zealand. *Proceedings 12th New Zealand Geothermal Workshop*, pp. 251-264. (1990).

Caine, J.S., Evans, J.P., Forster, C.B.: Fault zone architecture and permeability structure. *Geology, 24*: 11, pp. 1025-1028. (1996).

Chiodini, G., Cardellini C., Amato A., Boschi E., Caliro, S., Frondini, F., Ventura, G.: Carbon dioxide Earth degassing and seismogenesis in central and southern Italy. *Geophysical Research Letter*, 31, L07615. (2004).

Chiodini, G., Cioni, R., Guidi, M., Raco, B., Marini, L.: Soil $CO_2$ flux measurements in volcanic and geothermal areas. *Applied Geochemistry*, 13(5), pp. 543-552. (1998).

Giammanco, S., Sims, K.W., Neri, M.: Measurements of $^{220}Rn$ and $^{222}Rn$ and $CO_2$ emissions in soil and fumarole gases on Mt. Etna volcano (Italy): Implications for gas transport and shallow ground fracture. *Geochemistry, Geophysics, Geosystems*, 8(10). (2007).

Giggenbach, W.F., Sheppard, D.S., Robinson, B.W., Stewart, M.K., Lyon, G.L.: Geochemical structure and position of the Waiotapu geothermal field, New Zealand. *Geothermics*, 23(5-6), pp. 599-644. (1994).

Grindley, G.W.: Sheet 8—Taupo. Geological map of New Zealand 1:250 000. Wellington, New Zealand. *Department of Scientific and Industrial Research*. (1960).

Grindley, G.W.: Geology and Structure of Waiotapu Geothermal Field. In Waiotapu Geothermal Field. NZ *Department of Scientific and Industrial Research Bulletin* 155, pp. 10-25. (1963).

Healy, J. and Hochstein, M.P.: Horizontal flow in hydrothermal systems. New Zealand, *Journal of Hydrology*, 12, pp. 71-82. (1973).

Healy, J.: Waiotapu geothermal field: Minerals of New Zealand (Part D-Geothermal Resources) *Report NZGS 38D, NZ Geological Survey*, Rotorua, NZ. (1974).

Hedenquist, J.W. and Henley R.W.: Hydrothermal eruptions in the Waiotapu Geothermal System, New Zealand: Their Origin, associated breccias, and relation to precious metal mineralization: *Economic Geology*, 80, pp. 1640-1668. (1985).

Hedenquist, J.W. and Browne, P.R.: The evolution of the Waiotapu geothermal system, New Zealand, based on the chemical and isotopic composition of its fluids, minerals and rocks. *Geochimica et Cosmochimica Acta*, 53, pp. 2235–2257. (1989).

Hinkle M, Kilburn J.: The use of vacutainer tube for collection of soil sample for helium analysis. *U.S. Geol. Surv. Open File Rep.* 79:1441. (1979).

Jolie, E., Klinkmueller, M., Moeck, I.: Diffuse Degassing Measurements as a Geochemical Exploration Tool: A Case Study From The Brady's Geothermal System (Nevada, USA). *Geotherm. Resour. Counc. Trans.*, 36, pp. 685-688. (2012).

Jolie, E., Klinkmüller M., Moeck I.: Diffuse surface emanations as indicator of structural permeability in fault-controlled geothermal systems. *Journal of Volcanology and Geothermal Research*, 290, pp. 97-113. (2015).

Jolie, E., Klinkmueller, M., Moeck, I., Bruhn, D.: Linking gas fluxes at Earth‘s surface with fracture zones in an active geothermal field. *Geology*, 44(4), pp. 187-190. (2016).

Kilgour, G., Blundy, J., Cashman, K. et al.: Small volume andesite magmas and melt–mush interactions at Ruapehu, New Zealand: evidence from melt inclusions. *Contributions to Mineralogy and Petrology*, 166, pp. 371-392. (2013).

Lamb, S. and Smith, E.: The nature of the plate interface and driving force of interseismic deformation in the New Zealand plate-boundary zone, revealed by the continuous GPS velocity field. *Journal of Geophysical Research: Solid Earth* 118, pp. 3160–3189. (2013).

Lee, H., Muirhead, J.D., Fischer, T.P., Ebinger, C.J., Kattenhorn, S.A., Sharp, Z.D., Kianji, G.: Massive and prolonged deep carbon emissions associated with continental rifting. *Nature Geoscience 9*, pp. 145–149. (2016).

Leonard, G.S., Begg, J.G., Wilson, C.J.N. (compilers): Geology of the Rotorua area: scale 1:250,000. Lower Hutt: *Institute of Geological and Nuclear Sciences Limited. Institute of Geological and Nuclear Sciences* 1:250.000 geological map 5. 102 p. + 1 folded map. (2010).

Mazot, A. and Christenson, B.W.: Tuneable Diode Laser for measuring CO2 and CO air concentration on New Zealand volcanoes: An emerging technique, *American*

*Geophysical Union, Fall Meeting 2012*, Abstract V21B-2769. (2012).

Mazot, A., Rae, A.J., Jentsch, A.: Detecting diffuse $CO_2$ emissions along the Ngapouri Fault using a tunable diode laser, *Proceedings 36th New Zealand Geothermal Workshop, Auckland, New Zealand.*, 6 p. (2014).

Myers, J., Kelly, T., Lawrie, C., Riggs, K.: Environmental Technology Verification Report, Boreal Laser Inc. GasFinder 2.0 Tunable Diode Laser Open-Path Monitor, *US EPA Archive Document*. (2000).

Nairn, I.A.: Geology of the Waimangu geothermal mapping project area, Central volcanic region, New Zealand. Unpublished report, *N.Z. Geological Survey*, Rotorua. (1973).

Nairn, I., Wood, C., Bailey, R.: The Reporoa caldera, Taupo Volcanic Zone: Source of the Kaingaroa ignimbrites. *Bulletin of Volcanology*, 56, pp. 529-537. (1994).

Newson, A.M., Pebble, W.M., Browne, P.R.L.: Landsliding at Paeroa Fault at Te Kopia, *Proceedings 24, NZ Geothermal Workshop.* (2002).

Parkinson, K.J.: An improved method for measuring soil respiration in the field. *J. Appl. Ecol. 18*, pp. 221-228. (1981).

Rowland, J.V., Wilson, C.J.N., Gravley, D.M.: Spatial and temporal variations in magma-assisted rifting, Taupo Volcanic Zone, New Zealand. *Journal of Volcanology and Geothermal Research,* 190, pp. 89-108. (2010).

Rowland J.V. and Sibson R.H.: Extensional fault kinematics within the Taupo Volcanic Zone, New Zealand: Soft-linked segmentation of a continental rift system. *New Zealand Journal of Geology and Geophysics,* 44, pp. 271-283. (2001).

Rowland, J.V. and Simmons, S.F.: Hydrologic, magmatic, and tectonic controls on hydrothermal flow, Taupo Volcanic Zone, New Zealand: implications for the formation of epithermal vein deposits. *Economic Geology*, 107, pp. 427–457. (2012).

Seebeck, H., Nicol, A., Villamor, P., Ristau, J., Pettinga, J.: Structure and kinematics of the Taupo Rift, New Zealand. *Tectonics*. 33, pp. 1178–1199. (2014).

Smith, L., Forster, C., Evans, J.: Interaction of fault zones, fluid flow, and heat transfer at the basin scale, in Selected Papers*: Hydrogeology, International Association of Hydrogeology,* Verlag Heinz Heise, Hannover, Germany. (1991).

Tronicke, J., Villamor, P., Green, A.G.: Detailed shallow geometry and vertical displacement estimates of the Maleme Fault Zone, New Zealand, using 2D and 3D georadar. *Near Surface Geophysics,* 4, pp. 155-161. (2006).

Trottier S., Gunter, W.D., Kadatz, B., Olson, M., Perkins, E.H.: Atmospheric Monitoring for the Pembina Cardium $CO_2$ Monitoring Project using Open Path Laser Technology. *Energy Procedia*, 1, pp. 2307-2314. (2009).

Villamor P. and Berryman K.: A late Quaternary extension rate in the Taupo Volcanic Zone, New Zealand, derived from fault slip data. *New Zealand Journal of Geology and Geophysics*, 44:2, pp. 243-269. (2001).

Wilson, C.J.N. and Rowland J.V.: The volcanic, magmatic and tectonic setting of the Taupo Volcanic Zone, New Zealand, reviewed from a geothermal perspective. *Geothermics,* 59, pp. 168-187. (2015).

West Systems: Carbon Dioxide Flux Meter, Handbook, Release 4.11. (2002)